INTERNAL WAVES DYNAMICS IN THE LOMBOK STRAIT STUDIED BY A NUMERICAL MODEL

NINING SARI NINGSIH, RIMA RAHMAYANI,
SOFWAN HADI AND IRSAN S. BROJONEGORO

Abstract A baroclinic ihrec-dimensional (3D) hydrodynamic model with ihe non-hydroslatic approximalion called Massachusetts Institute of Technology - Global Circulation Model (MlTgcm) has been applied to simulate the generation of internal tidal bores and their disintegration into internal solitary waves in the Strait of Lombok. Numerical simulations have been carried out by incorporating seasonal variations of the stratification of [he water body, which exist during the 1" transitional monsoon, the east monsoon, the 2^{M} transitional monsoon, and the west monsoon. Our simulation yields the results that the existence of the sill at the southern part of the Lombok Strait, strong tidal flow, and a stratified fluid, play an important role in forming some short of divergence and convergence area as an indication of the birth of internal waves, which are simulated on the both sides of thcsill. The simulated results reproduce reasonably well the basic features of internal waves in the Strait of Lombok as captured by the Synthetic Aperture Radar (SAR) from the European Remote Sensing (ERS) satellites ERS I and ERS 2, such as a north-south asymmetry, propagation speeds, average amplitudes and wavelengths, and soliton packets. Similar to observations made by National Oceanic and Atmospheric Administration (NOAA) satellites, the simulation results also showed the intrusion of warm water from the Pacific Ocean into the Indian Ocean and the existence of well-developed thermal plume at south of the sill. Seasonal variations of interface depth of thermocline and the density difference between the stratified layers influence magnitudes of the amplitudes and wavelengths of the internal waves and solitons, and the distance of thermal plume in the Lombok Strait. It is found that during the monsoon transition periods and the west monson, ihe amplitudes of internal waves and solitons at the southern part of the strait is apparently larger than those at the northern one, whereas during the east monsoon, the wave amplitudes is larger north of the sill than south of it. Meanwhile, the propagation speeds *of* northward propagating internal solitary waves (0.71 -2.67 m/s) arc stronger than southward propagating ones(0.21-1.53 m/s) throughout the monsoon periods.

Keywords: internal waves, non-hydrostatic approximation, solitary waves, thermal plumes.

1. Introduction

Internal waves are motions that occur beneath the free-surface of a density-stratified water body, which carry energy and momentum through a basin and contribute to mixing events in littoral regions that prompt changes of marine ecosystem. As an external force (i.e., wind, river inflow, and tides) moves the density layers from their equilibrium position, an internal wave is initiated to restore the system to equilibrium. Internal waves propagate through the basin and interact with the basin boundaries;* this internal wave - slope interaction is an important source of energy that transports CO„ nutrients, biota and contaminants through the water column (Imberger and Ivey, 1993; Javame/a/.. 1999).

[1] ProoamSiud>orOccanography.LabTckXlBuilding. I'Floot.BandungInsltluicofTcchnolugy. JlGmciha 10, Bandung 40132, Indonesia. • E-mail: niningggn.ph.iib.acjj
' *ftDcaixMtitt>ai Bremen* University. Germany
' Program Study of Ocean Engineering, Bandung Institute of Tcdinology

Biogeochemical processes in oceans, lakes, and estuaries evolve against the background of vertical density stratification. One of the most important parts of the biogeochemical processes in the oceans is the CO, cycle, which plays an important role in the mechanism of global warming.

The subject of internal waves interacting with bottom topographic features in the ocean has received much attention in the past few decades. This is mainly attributed to a proposition that instabilities and breaking of internal waves at boundaries can be a significant source of turbulence, leading to mixing and transport in the ocean (Munk and Wunsch, 1998). Amplitudes (peak to through) of internal waves in several seas may exceed 30 m, such as ±40 m in Andaman Sea(Massel, 1999), ±90 m in Gibraltar Strait (Bockel, 1962), and >I00 m in the Lombok Strait (Susanto *el al.,* 2005). Regarding to estimation of the internal wave energy, researchers from University of Washington - USA have determined the direction of the internal waves and their strength in terms of kilowatts per meter of ridge length (http://unisci.com), namely about 5 to 10 kilowatts per meter along the Hawaiian Ridge, more than 40 kilowatts per meter over the submerged Kaena Ridge off western Oahu, and about 60 kilowatts per meter measured at the French Frigate Shoals 400 miles northwest of the Hawaiian Islands.

Most of the internal wave studies were carried out by using field measurements of physical sea water properties and SAR images. Packets of internal waves acquired from satellite images are often covered by clouds, so that it is difficult to monitor the spatial and temporal variability of the internal waves. In addition, field measurements of oceanographic parameters to predict internal waves need high cost. By considering the constraints of both methods, in this paper we address to study internal waves by using a numerical model. With the development of both computer and numerical methods for solutions of time-dependent flows, numerical simulation has become an economic and effective way to obtain the required, flow parameters compared to the high cost of performing field observations.

According to Brandt *el at.* (1997), when modeling internal waves, the problem can be separated into a "generation phase" and a "propagation phase". In a "generation phase", the hydrostatic approximation is usually applied (Hibiya, 1986, 1990; Longo *el* «/.. 1992). Here, the hydrostatic "generation phase" describes the dynamics of the water masses in the region near to sill where the internal bores are generated. Meanw hile, a non-hydrostatic one is required for a "propagation phase" (Gerkema and Zimmerman, 1995; Brandt *etal.,* 1996). The non-hydrostatic "propagation phase" describes the dynamics of the water masses outside the generation region where the internal bores may disintegrate into internal solitary waves.

In general, large-scale ocean and littoral modeling have traditionally made the hydrostatic approximation, which neglects non-hydrostatic pressure and subsequently vertical momentum. A typical hydrostatic ocean model applies a spatial grid with an aspect ratio (Az/Ax) of 0(10"), where Az and Ax are vertical and horizontal grid spacing, respectively. Hence, typical value of vertical velocity is small compared to the horizontal one, so that the vertical acceleration can be neglected. The hydrostatic approximation fails at open boundaries and at steep slopes with strong vertical velocities. Linear waves that arc damped by viscous effects may be considered to behave hydrostatically, while internal waves that steepen nonlinearly are inherently non-hydrostatic. It is suggested that non-hydrostatic pressure is essential for proper modeling of internal wave development and propagation (Wadzuk. 2004). Therefore, this new- development of non-hydrostatic approximation is of particular importance for a comprehensive investigation of generation and propagation

of internal waves.

In our previous study, as preliminary investigation, we have carried out simulation of internal wave generation in the Lombok Strait by using the hydrostatic approximation (Ningsih *et al.*, 2004). As an extension of this study, we have investigated the propagation of internal waves in the Lombok Strait by applying a non-hydrostatic approximation. So that, the dynamics of the water masses outside the generation region where the internal bores may disintegrate into internal solitary waves as captured by SAR images will be able to be simulated by the model.

2. Hydrodynamics of the Strait of Lombok

The Strait of Lombok separates the Bali Island from the Lombok Island and connects the Flores Sea in the north with the Indian Ocean in the south. The Lombok Strait plays an important role in transporting the huge flow of warm, low salinity water from the Pacific Ocean into the Indian Ocean as pan of the Indonesian throughilow (ITF), in which the flow having a large impact on the global climate system. The strait is not only important as one of the routes of the ITF, but also it serves as a navigation route for international ships as well as the national ones, such as submarines of the naval army and trade ships. While in the southern part of the strait the water depth increases rapidly (a depth of 2500 m is encountered approximately 35 km south of the sill), in the northern part it increases more gently (a depth of 1250 m is encountered approximately 35 km north of the sill).

In the southern part of the strait, the channel is divided into two by the smal I Nusa Penida Island. The channel at the western part of this island (Badung Strait) only has a cross sectional area less then one-fourth of the main channel and its water depth is less than 100 m. The eastern channel is deeper, connects Nusa Penida Island with the lombok Island, and has a sill with a maximal depdi of 350 m and a length of 20 km. In the southern part of the strait the huge amount of water flowing from the Pacific Ocean into the Indian Ocean, sometimes more than 4 million cubic meters of water per second, is pushed over the sill causing a large speed current (Visser, 2004). In addition, due to topographic constrictions, tidal current velocity in the Strait of Lombok can attain values as high as 3.5 m/s in the sill region (Murray and Aricf. 1988; Murray *et al.*, 1990).

The tide in the Lombok Strait is produced by tidal waves from the Indian Ocean; and at the sill region, it is predominantly semi-diurnal. However, the tide in the northern part of the Lombok Strait is predominantly diurnal cycle and tidal current amplitudes there range from 0.20 to 0.50 m/s (Murray and Arief, 1988)

During most of the year, a seasonal thermocline is present in the strait. Together with a large tidal current and the presence of stratified water, one can imagine that the huge amount of water flow passing the sill can lead to large oceanographic phenomena, such as internal wave generation, mixing, and transport mechanisms in and around the Lombok Strait. More detailed information on the hydrodynamics of the Strait of Lombok can be found in Murray and Arief (1988), Arif (1992), Arif and Murray (1996). and Hautala *et al* (2001).

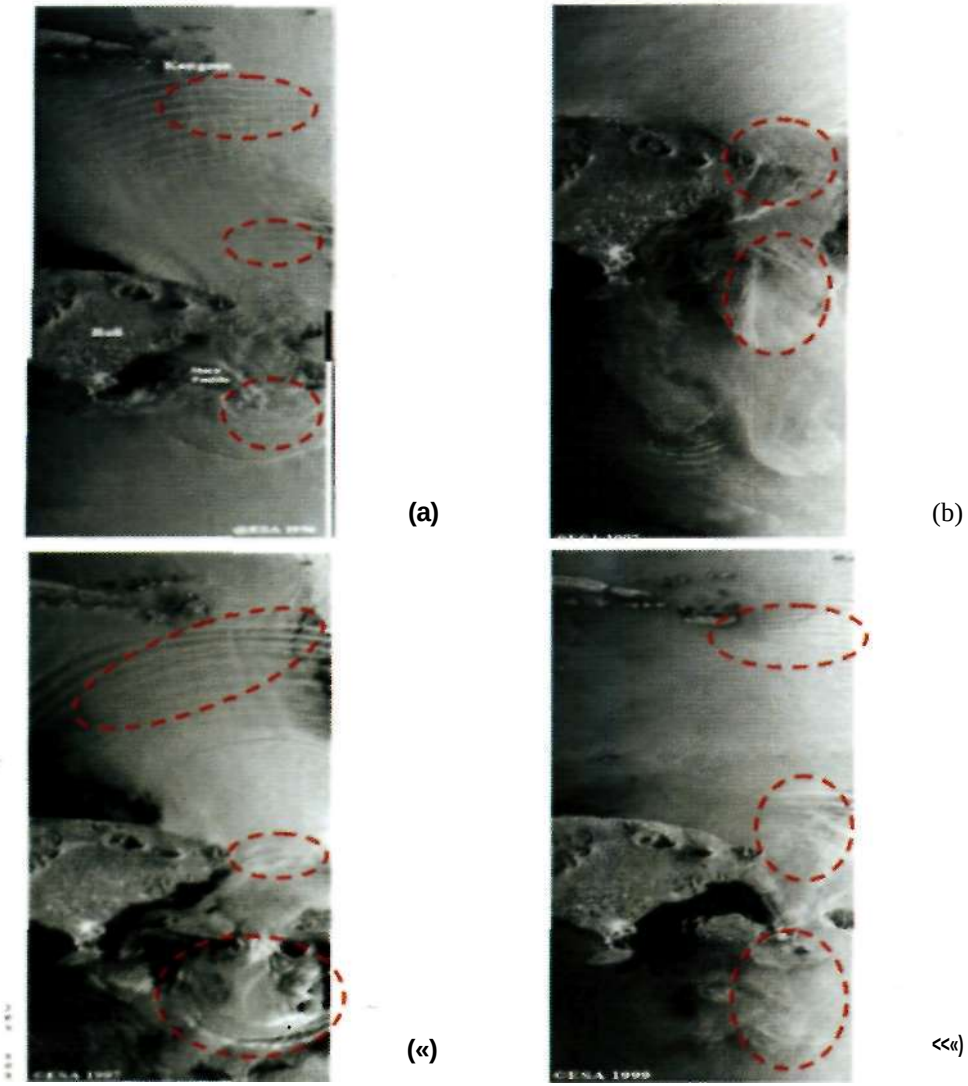

Figure 1. ERS-l/2imagesoftheStraitofLombokwereacquiredat02:32UTC:(a).on23April 1996, (b). on 27 August 1997, (c). on 5 November 1997, and (d). on 15 December 1999, respectively (Susanto *etal,* 2005 and Mitnik *et al.,* 2000).

3. Observation of Internal Solitary Waves

In the previous study (Mitnik *et al.,* 2000; Mitnik and Alpers, 2000; Ningsih *et al.,* 2004; Susanto *et al.,* 2005), it was suggested that the internal solitary waves in the Lombok Strait were generated in stratified water by tidal currents in the sill area between the Nusa Penida and Lombok Islands. In addition, Susanto *et al.* (2005) concluded that background current (i.e., the ITF), tidal conditions, stratifications control the internal-wave generation and propagation in the Strait of Lombok.

Several observation of internal solitary waves generated in the Strait of Lombok was made by the SAR from the ERS 1 and ERS 2 satellites. Figure 1 shows ERS-1/2 images, which were acquired at 02:32 UTC on 23 April 1996, on 27 August 1997, on 5

November 1997, and on 15 December 1999, respectively (Susanto *et al.*, 2005 and Mitnik *et al.*, 2000). The period of the SAR images were chosen to represent typical times of the west-east transitional monsoon, the east-monsoon, the east-west transitional monsoon, and the west-monsoon in order to investigate characteristics of internal waves and their variation in the Lombok Strait. The images in Figure 1 show clearly sea surface manifestations of packets of internal solitary waves (circular bright/dark patterns) propagating both southward and northward. Susanto *et al.* (2005) have calculated the dynamical parameters of the northward-propagating internal waves in the Strait of Lombok by analyzing two consecutive satellite SAR images acquired on April 23 and 24, 1996. They reported that the average propagation velocity of northward-propagating internal solitary wave trains in the Strait of Lombok is 1.96 m/s, the average wavelength is about 3.8 km, and solitons in a packet are about 23. Meanwhile, during an oceanographic cruise of International Nusantara Stratification and Transport (INSTANT) Indonesian throughflow from June to July 2005, Susanto *et al.* (2005) detected large amplitude isolated signal of internal solitary waves propagating northward that were recorded by an EK500 Echosounder in the Lombok Strait (115.75 °E, 8.47 °S). These waves have wavelengths of ~1.8 km and their amplitude (peak to trough distance) exceeds 100 m.

4. Model **Description and Its Application**

4.1. Governing Equations

Simultaneous satellite SAR sensing, measurement data, and numerical models can be used to estimate characteristics of internal waves as well as to calculate tJieir dynamic parameters. In this study, in order to describe and to predict the dynamics of water masses and internal waves in the Lombok Strait, we have carried out numerical simulations of their dynamics by applying a baroclinic three-dimensional ocean circulation model called MITgcm described by Hill and Marshall (1995), Marshall *et al.* (1997), Adcroft *et al.* (1997), Adcroft and Marshall (1999), Marotzke *et al.* (1999); Adcroft and Campin (2004), Adcroft *et al.* (2004), and Marshall *et al.* (2004). The governing equations used in the model are the semi-compressible Boussinesq equations. The MITgcm was selected because it has non-hydrostatic capability in the Boussinesq equations and so can be used to study both the generation of internal tidal waves and their disintegration into internal solitary waves.

The system of equations with the semi-compressible Boussinesq and non-hydrostatic approximation in z-coordinate are given by:

The continuity equation:

$$\nabla_h . \vec{v}_h + \frac{\partial w}{\partial z} = 0 \qquad (1)$$

The horizontal momentum equation:

$$\frac{D\vec{v}_h}{Dt} + f\hat{k} \times \vec{v}_h + \frac{1}{\rho_c} \nabla_h p' = \vec{F}_{\vec{V}} \qquad (2)$$

The vertical momentum equation:

$$\epsilon_{nh} \frac{Dw}{Dt} + \frac{g\rho'}{\rho_c} + \frac{1}{\rho_c} \frac{\partial p'}{\partial z} = \epsilon_{nh} F_w \qquad (3)$$

The equation of state:

$$\rho' = \rho\left(\theta, S, p_o(z)\right) - \rho_c \qquad (4)$$

The equation of potential temperature transport:

$$\frac{D\theta}{Dt} = Q_\theta \qquad (5)$$

The equation of salt transport:

$$\frac{DS}{Dt} = Q_s \qquad (6)$$

where $\vec{v}_h$ is the horizontal component of velocity (m/s); w is the vertical velocity (m/s); t is time (s); f is the Coriolis parameter (rad/s); ρ_c is a constant reference density of water (kg/m^3); ρ' is variation of density (kg/m^3); p' is variation of pressure (kg.m^{-1}.s^{-2}); $\vec{F}$ are forcing and dissipation of $\vec{v}$ per unit mass (m/s^2); F_w are forcing and dissipation of w per unit mass (m/s^2), θ is potential temperature (°C), S is Salinity (PSU), $p_o(z)$ is a reference pressure (kg/m^3), Q_θ are forcing and dissipation of θ (°C/s), Q_s are forcing and dissipation of S (PSU/s), and $\in_{nh}$ is a non-hydrostatic parameter (coefficient).

where v_h is the horizontal component of velocity (m/s); w is the vertical velocity (m/s); f is time (s); / is the Coriolis parameter (rad/s); p_c is a constant reference density of water (kg/m^3); p'is variation of density (kg/m^3); p' is variation of pressure (kg.m'".s"~); Fare forcing and dissipation of v per unit mass (m/s^2); F_w are forcing and dissipation of w per unit mass (m/s^2), *6* is potential temperature (°C), Sis Salinity (PSU), $p_o(z)$ is a reference pressure (kg/m^3), Q_g are forcing and dissipation of *6* (°C/s), _>, are forcing and dissipation of S (PSU/s), and e_{nh} is a non-hydrostatic parameter (coefficient).

4.2. Model Parameters

In this study, to reduce the large amount of computational grids in the model domain, we approximate the computational domain and bottom topography of the Strait of Lombok with a uniform channel width only, but it retains.the feature of its bottom topography by including a realistic depth profile, as plotted in Figures 2a and more resolution near the interface depth of the stratified water (thermocline). The vertical grid spacing ranges from approximately 50 m in the interface depth to about 150 m near the bottom.

In this study, the ocean circulation system is forced by imposing tidal displacements at the northern and southern boundaries. The values for elevation used at the two open boundaries were a combination of M_2, S_2, N_2, K_2, K_t, Oi, Pi, I and Qi tidal elevations derived from the tide model driver (TMD) of Padman (2005). In order to minimize reflections at the open boundaries, the Sommerfeld radiation condition (Chapman, 1985) was implemented in the model to represent the flow velocity at these open boundaries.

As mentioned in section 1, it is quite likely that internal waves appear along the density gradients within the ocean and the I largest frequency for the internal waves occur in the thermocline. In order to better I understand the dynamics of internal waves I and their variation in the Lombok Strait, I four different numerical simulations with I different parameters of the thermocline I locations of the stratified fluid and of the I density difference between the water layers • have been carried out in this study. The I four different numerical simulations refers I to scenarios in which the seasonal I thermocline is present in the Strait of I Lombok, namely associated with the west- I east transitional monsoon (the 1^{sl} 1 transitional monsoon), the east-monsoon, I the east-west-transitional monsoon (the 2nd I transitional monsoon), and the west- I monsoon, respectively. For simplicity, in I this study we considered the density I difference between the water layers only I caused by the difference in temperature. I Here, we neglected the spatial and temporal I variability of salinity.

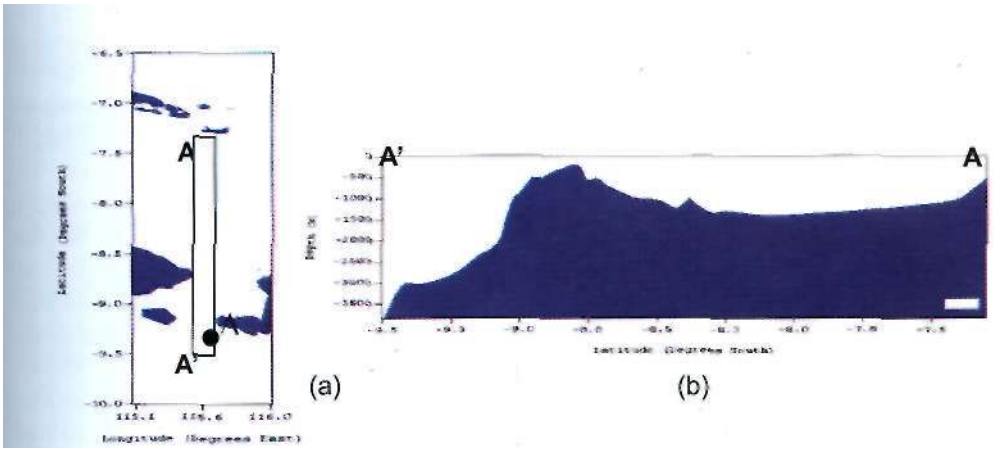

Figure 2. Topography of the Strait of Lombok used in the simulations. The channel width is depicted in (a) and the depth profile in (b). Tidal condition at Location of a dark circle (marked by •) is selected as the reference time of the flood and ebb conditions. A triangle (marked by A) is location of tidal gauge in Lembar.

Table 1. Typical values of parameters, characterizing the water stratification, used as initial values in the numerical model associated with the monsoon climate. Here, *h*, (m) is the thermocline depth and *Ap* (kg/m^3) is averaged values of density difference along locations of thermocline.

	The 1^{sl} transitional monsoon	The east-monsoon	The 2nd transitional monsoon	The west-monsoon
In the northern part of the Lombok Strait	*h*, = 175 *Ap* = 3.689	*h*, = 150 *Ap* =3.614	*h*, • 225 4/3=3.610	*h*, = 250 *Ap* = 3.876
In the southern part of the Lombok Strait	*h*, = 175 *Ap*= 3.429	*h*, = 150 Zips 3.639	*h*, = 225 *Ap* =3.491	*h*, = 250 4p=3.314

Initial values of the temperature and the interface depth were specified by the Levitus data of WOA98 (http://iridl.ldeo.columbia.edu). Temperature is also specified along the open boundaries. If the flow is directed out of the domain, the interior values are simply advected out of the domain. When outflow turns to inflow, the water property values move toward specified values, which were specified by the the Levitus data of WOA98. Table 1 shows typical values of parameters, characterizing the water stratification, used as initial values in the four scenarios of simulation associated with the monsoon climate that exists in the Lombok Strait. Each scenario of simulation associated with monsoon condition was carried out by running the model for several tidal cycles which cover both the period of spring and neap tides (+15 days) and of the available SAR images representing each seasonal climatology as shown in Figure 1, so that the comparison of our numerical simulations with the results of the available ERS-1/2 SAR data could be performed.

5. Simulations of Internal Waves in the Lombok Strait and Comparison with ERS-1/2 SAR IMAGES and Observed Data

Our simulation yields the results that the current circulation pattern in the Lombok Strait is generally associated with the prevailing tides in the Indian Ocean. During high tides, the current flows from the Indian Ocean into the strait. Otherwise, during low tides, the current flows

southward into the Indian Ocean (Figures 3 and 4). In this study, we have carried out verification by comparing the simulation results of elevation induced by the tide-driven circulation with those of tide-gauge data from Lembar as reported by Susanto *et al.* (2005). The verification is shown in Figure 5 and it can be clearly seen from the figure that the tidal type around the sill region is mixed (semidiurnal and diurnal tides).

In addition to the general circulation pattern described above, the numerical simulation results also show the existence of some short of divergence and convergence area as an indication of the birth of internal waves (Figures 6-9). In this study, the manifestations of the passage of the internal waves are also indicated by the movement of points of equal temperature (isotherms) or the agitation of the isotherm from its initial state. Due to the presence of the sill, the vertical component of the current periodically pulls down or lifts up the isotherm. The disturbance of the isotherm at this sill will then generate internal bores. During the propagation of the internal bores, they may disintegrate and thus give birth to a train of internal solitary waves (solitons). Our simulation results, carried out with different values of the stratification parameters representing the seasonal variations, can reproduce the generation of the internal solitary wave trains and their propagation northward as well as southward.

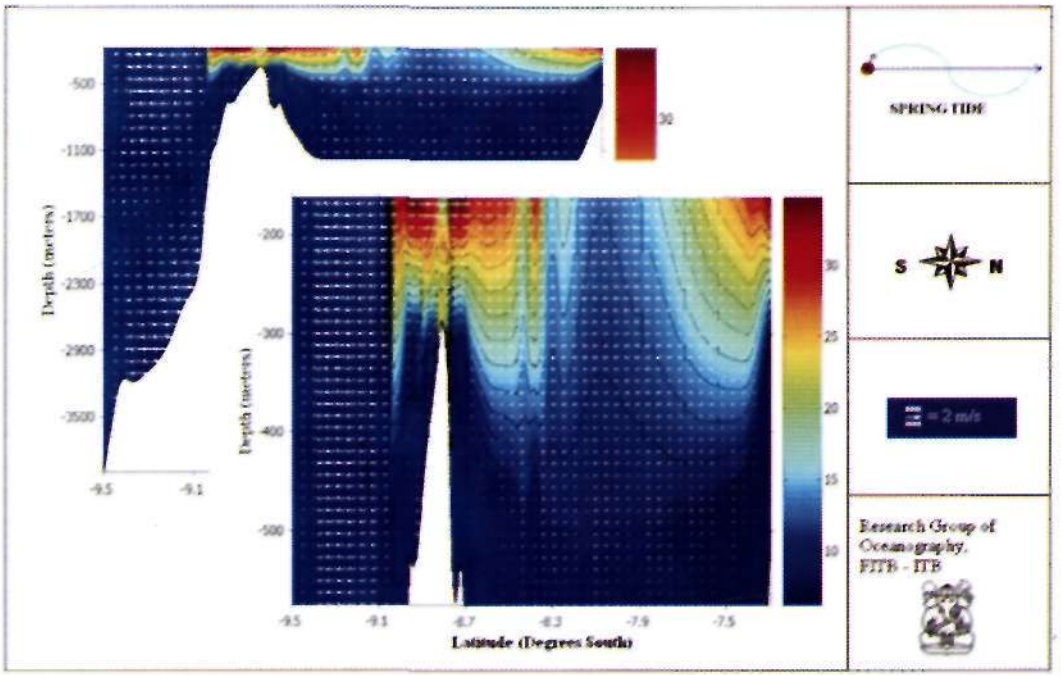

Figure 3. The flow regimes across the sill and the curve of isotherm for spring flood condition (during the east monsoon).

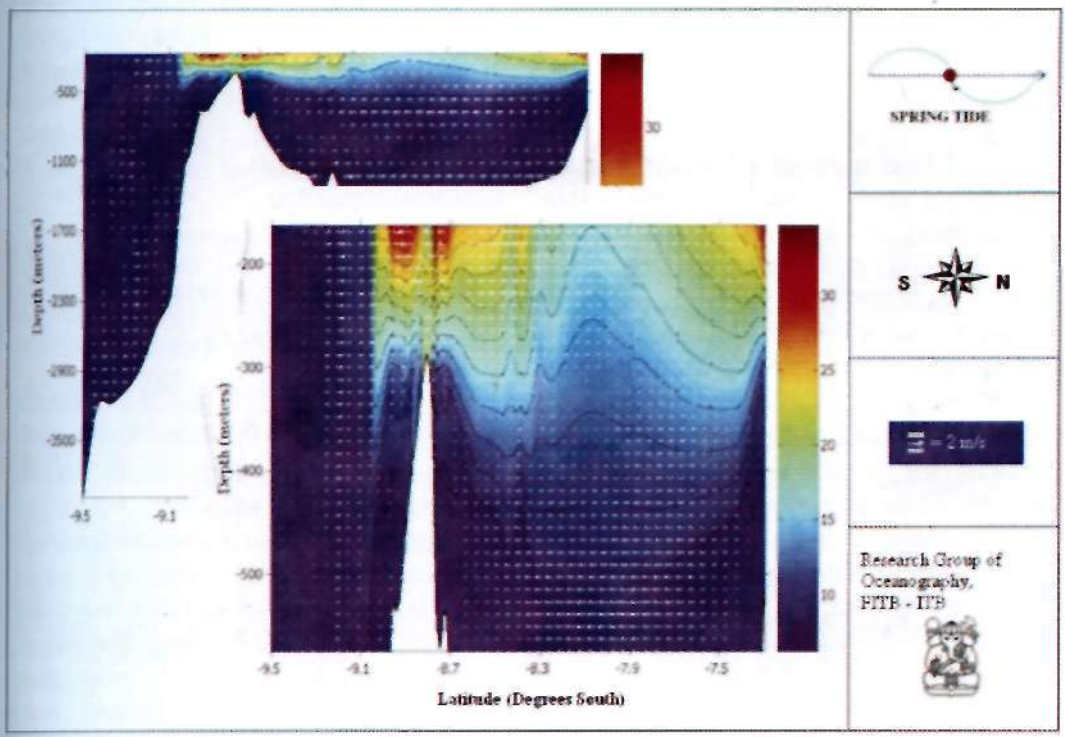

Figure 4. The flow regimes across the sill and the curve of isotherm for spring ebb condition (during the east monsoon).

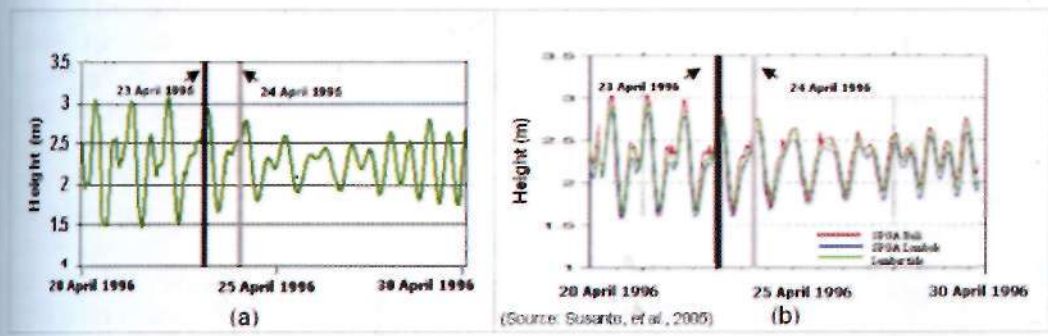

Figure 5. Verification of free surface elevation between (a) the simulation results and (b) observed tidal data (Source : Susanto *et al.*, 2005) in Lembar (marked by in Figure 2).

Figures 6-9 show space evolution of the interface between the stratified layers, representing internal solitary waves, as calculated with the numerical model in the case of the west-east transitional monsoon, the east monson, the east-west transitional monsoon, and the west monsoon, respectively. The arrows indicate the direction and the strength of the water flow.

Dynamical parameters of these simulated internal waves and internal solitary waves (Figures 6-9) are summarized in Table 2.

During the monsoon transition periods and the west monson (Figure 6-9, and Figures 8-9), the disturbance of isotherm south of the sill region is apparently stronger than that north of it. This means

that the amplitudes (peak to trough) of internal waves and solitons in the southern part of the strait are apparently more significance than in the northern one because the depth profile is steeper south of the sill than north of it. In addition, as the vertical density gradients (the water stratification) in the southern part of the strait are generally smaller than those in the northern one (Table 1), required energy to move water particles vertically is smaller south of the sill than north of it. Therefore, the amplitudes of internal waves and solitons at the southern part of the strait (the internal wave amplitudes are about 90-285 m; the soliton amplitudes are about 30-88 m) is larger than those at the northern one (the internal wave amplitudes are about 50-78 m; the soliton amplitudes are about 25-81 m), as shown in Table 2. However, during the east monsoon (Figure 7), the wave amplitudes is larger north of the sill than south of it (Table 2). Although the depth profile is steeper south of the sill than north of it, during the east monsoon the vertical density gradient in the northern part of the strait are smaller than that in the southern one (Table 1). Hence, during the east monsoon, the wave amplitudes in the northern region (the internal wave amplitude is about 300 m; the soliton wave amplitudes are about 60-80 m) is larger than those in the southern one (the internal wave amplitude is about 64 m; the soliton wave amplitudes are about 20-80 m). In general, during the west monson and the monsoon transition periods (the east monsoon), the larger (smaller) wave amplitudes south of the sill than north of it causes the shorter (longer) their wavelength south of the sill than north of it.

Our numerical simulations show that the phase speeds of the northward propagating internal waves trains (0.71-2.67 m/s) are faster than those of the southward one (0.21-1.53 m/s) throughout the monsoon periods. These simulated results agree well with those investigated by Susanto *et al.* (2005) and the relationship calculated analytically with the equation of the two-layer approximation (Bishop, 1984), which is usually expressed as

$$e\text{-}H*?)\text{-}Pffi\nearrow$$

where h_x is the depth of density interface (usually the thermocline), g is gravity, /?, is the density of the upper fluid, and p_2 is density of the lower fluid. Table 3 shows an example of averaged values of propagation speeds of southward- and northward-propagating internal waves trains in the Strait of Lombok calculated with the equation (7); here, the slower speeds of the southward propagating waves indicates that the Indian Ocean stratification is less intense from that of the northern part of the Lombok Strait.

The simulated results of characteristics of internal waves in the Lombok Strait agree at least qualitatively with the results of the available ERS 1⁄2 SAR data analyzed by Mitnik *et al.,* 2000 and Susanto *et al.,* 2005. In addition, our simulation results can also reproduce the presence a well-developed thermal plume south the sill, which is intruded into the Indian Ocean, as identified on several ERS SAR images by Mitnik *et al.* (2000). Moreover, our simulation present the large seasonal variations of the location of the front associated with this Pacific water plume south of the Lombok Strait (Figures 6-9 and Table 2). Mitnik *et al.* (2000) reported that the extent and shape of the thermal plume are determined by the water transport through the strait and characteristics of the South Java Current which in turn depend both local and remote atmospheric forcing, such as the annual cycle of the monsoon winds and

prolonged disturbances in wind field. For the comparison of our numerical simulations of dynamical parameters of southward- and northward-propagating internal waves in the Strait of Lombok with those investigated by previous scientists, we provided a summary of their dynamic parameters in Table 4.

Table 2. Dynamical parameter of southward- and northward-propagating internal waves and internal solitary waves in the Strait of Lombok.

	Internal Waves		Solitons				Southward Distance of Thermal Plumes from the Sill (km)
	Amplitude (peak to trough) (m)	Wave-length (λ) (km)	Amplitude (peak to trough) (m)	Wavelength (λ) (km)	Solitons in a Packet	Propa-gation Speeds (m/s)	
West-east Tansitional Monsoon	285 (S) 78 (N)	14.6 (S) 33.4 (N)	30-88 (S) 25-81 (N)	0.9-7.1 (S) 0.9-10.8 (N)	7-10 (S) 9 (N_1) 10 (N_2) 6 (N_3)	0.27-1.44 (S) 0.77-2.67 (N)	32.1
East Monsoon	64 (S) 300 (N)	14.6 (S) 10.9 (N)	20-80 (S) 60-80 (N)	0.3-11.6 (S) 0.9-14.6 (N)	6 (S) 10 (N_1) 5 (N_2) 8 (N_3)	0.21-0.69 (S) 2.46 (N)	29.9
East-west Tansitional Monsoon	250 (S) 50-60 (N)	15.8 (S) 75.4 (N)	80 (S) 64 (N)	1.64-7.6 (S) 2-10.4 (N)	10 (S) 10 (N_1) 12 (N_2) 5 (N_3)	0.28-1.53 (S) 1.72-2.66 (N)	66.2
West Monsoon	90 (S) 50 (N)	12.4 (S) 90 (N)	80 (S) 63 (N)	3.6-5.5 (S) 6.3-8.7 (N)	10 (S) 10 (N_1) 12 (N_2) 6 (N_3)	0.3-0.98 (S) 0.71-2.58 (N)	42.6
Notes:	*N: north of the sill, S: south of the sill, N_1: the first packet of the northward-propagating solitons, N_2: the second packet of the northward-propagating solitons, and N_3: the third packet of the northward-propagating solitons*						

Table 3. Averaged values of propagation speeds of soudiward- and northward-propagating internal waves trains in the Strait of Lombok calculated with the equation (7).

	West-east Tansitional Monsoon	East Monsoon	East-west Tansitional Monsoon	West Monsoon
North of the sill	$\Delta\rho$ = 3.2834 kg/m^3 h_1 = 94 m C = 1.72 m/s	$\Delta\rho$ = 3.2170 kg/m^3 h_1 = 70 m C = 1.47 m/s	$\Delta\rho$ = 3.2015 kg/m^3 h_1 = 171 m C = 2.29 m/s	$\Delta\rho$ = 3.416 kg/m^3 h_1 = 187 m C = 2.47 m/s
South of the sill	$\Delta\rho$ = 3.1077 kg/m^3 h_1 = 87 m C = 1.61 m/s	$\Delta\rho$ = 3.2866 kg/m^3 h_1 = 70 m C = 1.46 m/s	$\Delta\rho$ = 3.1168 kg/m^3 h_1 = 145 m C = 2.08 m/s	$\Delta\rho$ = 3.0822 kg/m^3 h_1 = 170 m C = 2.24 m/s

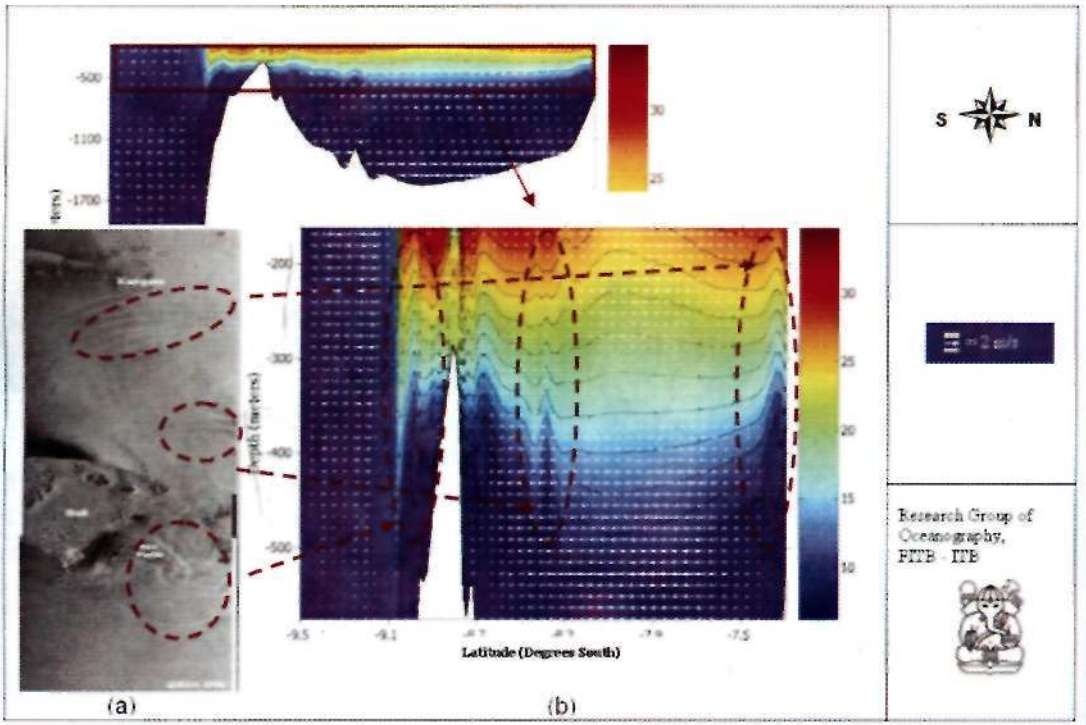

Figure 6. (a). ERS-1/2 images of the Strait of Lombok were acquired at 02:32 UTC on 23 April 1996. The image shows sea surface manifestation of packets of internal solitary waves propagating both northward and southward; (b). Space evolution of the interface between the stratified layers, representing internal solitary waves, as calculated with the numerical model in the case of the west-east transitional monsoon.

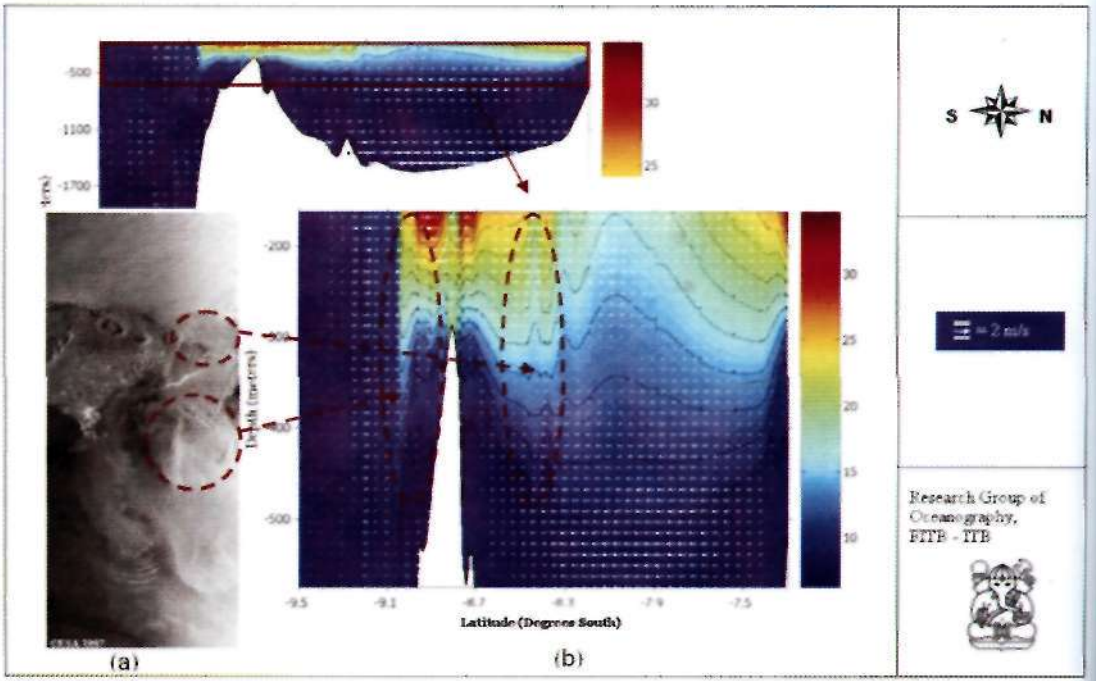

Figure 7. As in Figure 6 but for (a). 27 August 1997; (b) the case of the east monsoon.

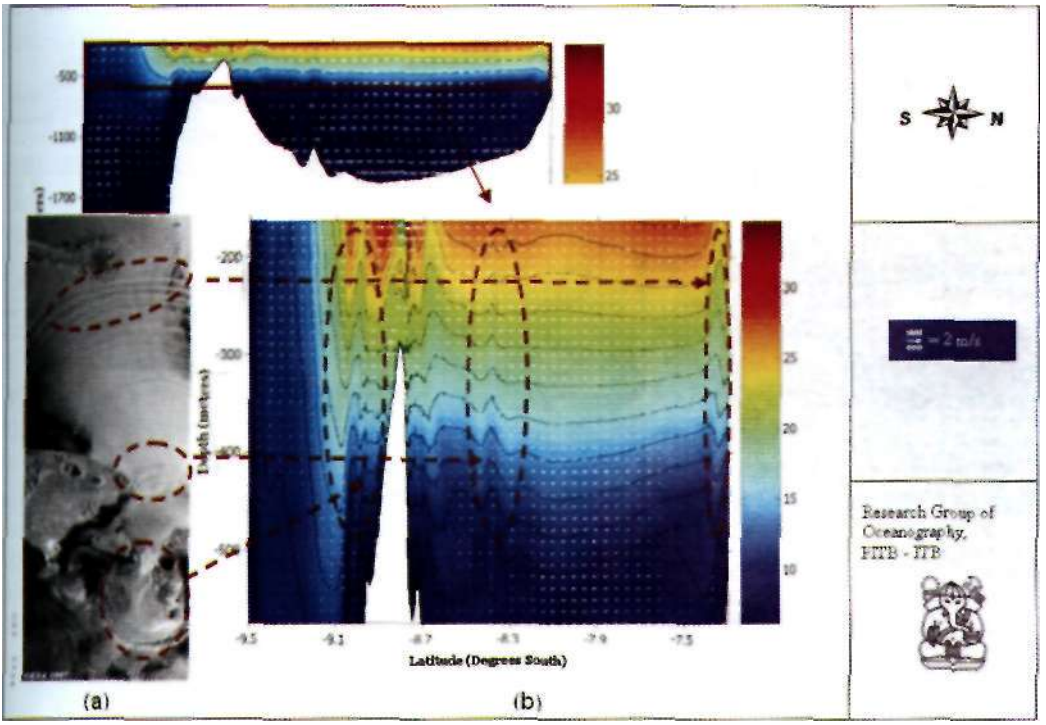

Figure 8. As in Figure 6 but for (a). 5 November 1997; (b) the case of the east-west transitional monsoon.

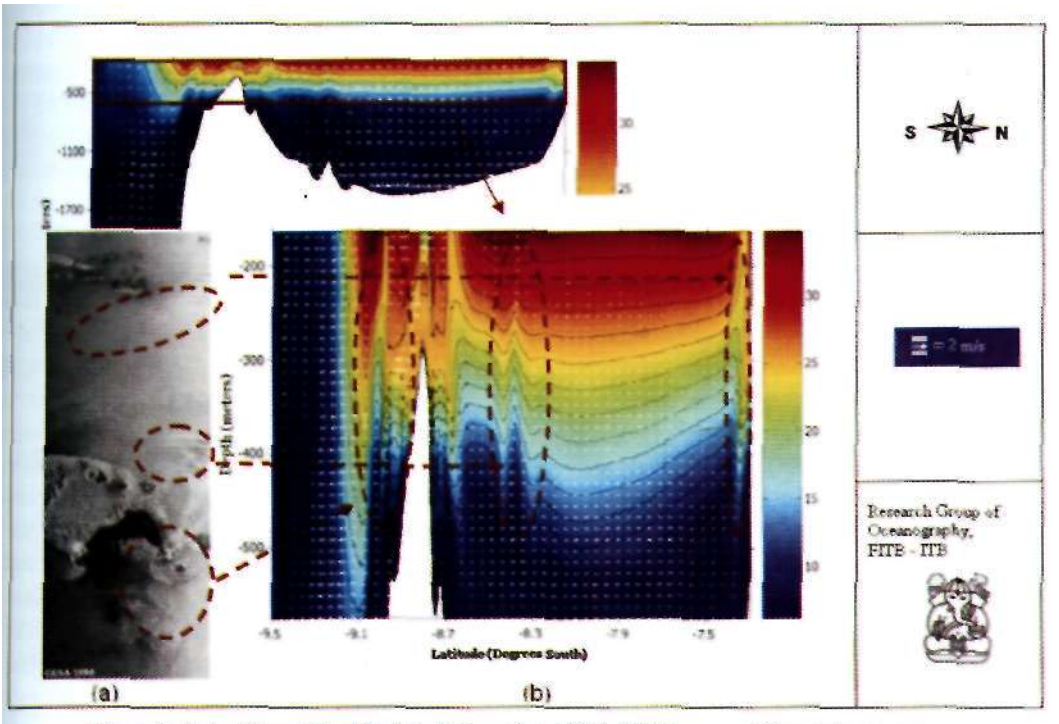

Figure 9. As in Figure 6 but for (a). 5 Desember 1999; (b) the case of the west monsoon.

Table 4. Dynamical parameters of southward- and northward-propagating internal waves in the Strait of Lombok, estimated in the present and past studies.

	Jaha-ruddin (2004)	Sulaiman (2004)	Susanto, *et al.* (2005)	Pujiana (2004); Ningsih, *et al.* (2004)	Visser (2004)	Mitnik, *et al.* (2000)	Present Study (Simulated by *MITgcm*)			
							West-east Transitional Monsoon (April)	East Monsoon (August)	East-west Tansitional Monsoon (November)	West Monsoon (Dec.)
Amplitude (peak to trough) of Internal Waves (m)			84-150 (S)	75-100 (S) 30-50 (N)			285 (S) 78 (N)	64 (S) 300 (N)	250 (S) 50-60 (N)	90 (S) 50 (N)
Wavelength of Internal Waves (λ), (km)				50-75			14.6 (S) 33.4 (N)	14.6 (S) 10.9 (N)	15.8 (S) 75.4 (N)	12.4 (S) 90 (N)
Amplitude (peak to trough) of Solitons (m)	39.45	25					30-88 (S) 25-81 (N)	20-80 (S) 60-80 (N)	80 (S) 64 (N)	80 (S) 63 (N)
Wavelength of Solitons (λ), (km)			1.4-2.5		1.863	Max 6.5 (Nov)	0.9-7.1 (S) 0.9-10.8 (N)	0.3-11.6 (S) 0.9-14.6 (N)	1.64-7.6 (S) 2-10.4 (N)	3.6-5.5 (S) 6.3-8.7 (N)
			1-3 2-5 2-7.5			0.7-2 (S) (Jan) 3.5-5 (N)				
						2-6.5 (N) (May)				
Solitons in a Packet			7-15 (S-N)			12 (N) (Nov)	7-10 (S) 9 (N_1) 10 (N_2) 6 (N_3)	6 (S) 10 (N_1) 6 (N_2) 8 (N_3)	10 (S) 10 (N_1) 12 (N_2) 5 (N_3)	10 (S) 10 (N_1) 12 (N_2) 6 (N_3)
			23-25 (April)			15 (N) (Dec)				
						14 (N) (May)				
Propagation Speeds of Solitons (m/s)			1.96-1.97		1.62	1.8-1.9 (Aug)	0.27-1.44 (S) 0.77-2.67 (N)	0.21-0.69 (S) 2.46 (N)	0.3-0.98 (S) 0.71-2.58 (N)	0.98 (S) 0.67-2.67 (N)
						2.5 (Dec)				
						2.5 (Jan)				
						1.9 (May)				
Notes:	*N: north of the sill, S: south of the sill, N_1: the first packet of the northward-propagating solitons, N_2: the second packet of the northward-propagating solitons, and N_3: the third packet of the northward-propagating solitons*									

6. Concluding Remarks

The generation of internal tidal bores and their disintegration into internal solitary waves in the Strait of Lombok and their relation to seasonal variations (monsoon) have been investigated by using the MITgcm model. The model results could confirm suggestion by previous investigators (e.g., Mitnik *et al.*, 2000; Ningsih *et al*, 2004; Susanto *et al*, 2005) that the internal solitary waves in the Lombok Strait are generated by the interaction of the tidal flow with the shallow sill located between the Nusa Penida and Lombok Islands. Generally, the characteristics of internal waves in the Lombok Strait obtained from the present simulation show a good agreement with the analysis of the available ERS 1/2 SAR

data of ihe Sirail of Lombok. which were carried oui by Milnik *el at.* (2000) and Susantoc/fl/.(2605).

The simulation results show that the stratification of the water body associated with monsoon climate and (he strength of the water flow through the strait play an important role in determining dynamical parameters of the internal waves in the Lombok Strait. Our simulation showed that (I) northward as well as southward propagating internal waves are generated in the Strait of Lombok, (2) during the monsoon transition periods and the west monson, the amplitudes of internal waves and solilons at the southem part of the strait are larger than those at the northern one, whereas during the east monsoon, the wave amplitudes are larger north of the sill than south of it (3) the phase speeds of the northward propagating internal waves trains are faster than those of the southward one throughout the monsoon periods.

In the present study, variation of the dynamic parameters of the internal waves in te Lombok Strait has been simply modelled, namely by approximating the computational domain with the uniform channel width, neglecting spatial and temporal variability of salinity, and by only considering tides as generating forces, whereas stratification effects and realistic geometry that exist in the Lombok Strait are likely to be complex and variable. In addition, very likely that both local and remote atmospheric forcing will control the internal-wave generation and propagation in this region. Therefore, idvanced modelling studies are necessary for more accurate calculation of dynamic parameters of the internal waves in the Strait of Lombok. namely by taking into account a realistic channel width, variability of saline stratification as well as the thermal one, background current associated with the ITF, and wind. As an extension of this research, thiskind of study iscurrently in progress.

References

Adcroft. A., C. Hill, and J. Marshall, 1997, Representation of topography by shaved cells in a height coordinate ocean model, Mon.Wea.Rev. 125:2293-2315.

Adcroft. A. and J. Marshall, 1999, A new treatment of the coriolis terms in c-grid models at both high and low resolutions. Mon.Wea.Rev. 127:1928-1936.

Adcroft, A. and J. M. Campin, 2004, Re-scaled height coordinates for Aaccurate representation of free-surface flows in ocean circulation models, Ocean Modelling 7:269-284.

Adcroft. A., J. M. Campin, C. Hill, and J. Marshall, 2004. Implementation of an atmosphere-ocean general circulation model on the expanded spherical cube, Mon. Wea. Rev. 132:2845-2863.

Arief, D., 1992, A study on low frequency variability in current and sea-level in the Lombok Strait and adjacent region, Ph.D. Dissertation, La. State Univ. at Baton Rouge.

Arief, D. and S. P. Murray, 1996, Low-frequency fluctuations in the Indonesian Throughflow through Lombok Strait", *J. Oeophys. Res.,* /0/f12,4S5-12,464.

Bishop, J. M., 1984. Applied oceanography, John Wiley & Sons, Inc.

Bockel. M., 1962, Traveaux oceanographiques de 'origny' a Gibraltar. CahiersOeonographique 14:325-329.

Brandt, P., W. Alpers, and J. O. Backhaus, 1996. Study of the generation and propagation of internal waves in the Strait of Gibraltar using a numerical model and Synthetic Aperture Radar images of the European ERS 1 Satellite, J. Geophys. Res. 101:14237-14252.3

Brandt, P., A. Rubino, W. Alpers, and J. O. Backhaus, 1997, Internal waves in the Strait of Messina studied by a numerical model and Synthetic Aperture Radar images from the ERS 1/2 satellites, J.

Geophys. Res. 27:648-663.

Chapman, D. C, 1985, Numerical treatment of cross-shelf open boundaries in a barotropic coastal ocean model. J. Phys. Ocean 15:1060-1075.

Gerkema, T. and J. T. F. Zimmerman, 1995, Generation of nonlinear internal tides and solitary waves, J. Geophys. Res. 25: 677-687.

Hautala, S. H., J. Sprintall, J. T. Potemra, J. C. Chong. W. Pandoe, N. Bray, and A. G. Ilahude, 2001, Velocity structure and transport of the Indonesian throughflow in the major straits restricting flow into the Indian Ocean, J. Geophys. Res. 106: 19527-19546.

Hibiya, T, 1990a. Generation mechanism of internal waves by a vertically sheared tidal flow over a sill, J. Geophys. Res. 95: 1757-1764.

Hibiya, T., 1990b, Generation mechanism of internal waves by tidal flow over a sill, J. Geophys. Res.9l: 7697-7708.

Hill, C. and J. Marshall, 1995, Application of a parallel Navier-Stokes Model to ocean circulation in parallel computational fluid dynamics in proceedings of parallel computational fluid dynamics: Implementations and results using parallel computers. Elsevier Science B.V. New York, 545-552.

Imberger. J. and G. N. Ivey,*1993. Boundary mixing in stratified reservoirs, J. Fluid Mech.~248:477-491.

Jaharuddin, 2004. Gelombang soliter di Selat Lombok dan simulasi numerik fenomena Morning Glory, Ph.D. dissertation, Bandung Institute of Technology, 2004. (Indonesian version).

Javam A., J. Imberger, S.W. Armfleld, 1999, Numerical study of internal wave reflection of sloping boundaries, J. Fluid Mech.396:183-301.

Longo. A.. M. Manzo. and S. Pierini, 1992, A model for the generation of nonlinear internal tides in the Strait of Gibraltar, Oceanol. Acta. 15:233-243.

Marotzke, J., R. Giering, K. Zhang, D. Stammer, C. Hill, and T. Lee, 1999, Construction of the adjoint MIT ocean general circulation model and application to Atlantic heat transport variability, J. Geophys. Res. 104(C12): 29529-29547.

Marshall, J., A. Adcroft, C. Hill, L. Perelman, and C. Heisey, 1997, A finite-volume, incompressible navicr stokes model for studies of the ocean on parallel computers, J. Geophys. Res. I02(C3): 5753-5766.

Marshall. J., A. Adcroft, J.M. Campin, C. Hill, and A. White, 2004, Atmosphere-ocean modeling exploiting fluid isomorphisms, Mon. Wca. Rev. 132: 2882-2894.

Masscl, S.R.. 1999, Fluid mechanics for marine ecologies. Springer-Verlag Berlin Heidelberg. Berlin.

Mitnik. L., W. Alpcrs. and H. Urn. 2000, Thermal plumes and internal solitary waves generated in the Lombok Strait studied by ERS SAR *in* ERS-Envisat Symposium: Looking down to earth in the new millennium, 16-20 October 2000. Gothenburg, Sweden. *SP-46L* European Space Agency, Publication Division, Noordwijk. The Netherlands, 1-9.

Mitnik, L. and W. Alpers, 200. Seal surface circulation through the Lombok Strait studied by ERS SAR *in* Proceedings of the 5 Pacific Ocean Remote Sensing

Conference (PORSEC 2000) I: 313-3l7,j Goa, India.

Munk. W. and C. Wunsch, 1998, Abyssal| recipes II: Energetics of tidal and wind mixing. Deep Sea Res., Part I 45: 1977-2010.

Murray, S. P. and D. Arief, 1988, Throughflow into the Indian Ocean through Lombok Strait, January 1985-January 1986. *Nature* 333:j 444-447.

Murray, S. P., D.Arief, J. C Kindle, and H.E. Hulburt, 1990, Characteristics of circulation in an Indonesian Archipelago Strait from hydrography, currents measurements and numerical model results, *in the Physical oceanography of straits*. Pratt, L. J., *(ed.)* Kluwer Academic Publishers, Norwell, MA, USA, 3-23.

Ningsih,N. S., S. Hadi, and K. Pujiana, 2004, *A numerical study of the generation of internal wave in the Lombok Strait, Paper* presented at International Nusantara Stratification and Transport (INSTANT) Workshop: Oceanography of Indonesian Seas, Bali, Indonesia.

Padman. L, 2005, Tide Model Driver (TMD) manual, Version 1.2, Earth & Space Research.

Pujiana, K., 2004, Dinamika gelombang internal di Selat Lombok, M.Sc. Thesis, Bandung Institute of Technology. (Indonesian version).

Sulaiman, A., 2004, Study of internal solitary wave by using satellite imagery and mathematical model. Proceedings of the thirteenth workshop of OMlSAR(WOM-13) on ihe Application and Networking of Satellite Data, Bali. Indonesia, 5 - 9 October 2004.

Susanto, R. D,, L. Mitnik, and Q. Zheng, 2005, Ocean internal waves observed in the Lombok Strait, Journal of Oceanography 18(4).

Visser, W. P., 2004. On the generation of internal waves in Lombok Strait throught Kelvin-Helmholtz Instability, M.Sc. Thesis, University of Twente.

Wadzuk, B. M.. 2004, Hydrostatic and non-hydrostatic internal wave models, Ph.D. Thesis, the University ofTexas, Austin.